Characterization of Actin- and Lipid-Binding Domains in Severin, a Ca^{2+}-Dependent F-Actin Fragmenting Protein†

Ludwig Eichinger and Michael Schleicher*
Max-Planck-Institut für Biochemie, 8033 Martinsried, Federal Republic of Germany
Received November 14, 1991; Revised Manuscript Received March 4, 1992

ABSTRACT: Severin is a Ca^{2+}-activated actin-binding protein that nucleates actin assembly and severs and caps the fast growing ends of actin filaments. It consists of three highly conserved domains. To investigate the domain structure of severin, we constructed genetically the N-terminal domain 1, the middle domain 2, and the tandem domains 2+3. Their interaction with actin, Ca^{2+}, and lipids was characterized. Domain 1 contains the F-actin capping and a Ca^{2+}-binding site [Eichinger, L., Noegel, A. A., & Schleicher, M. (1991) *J. Cell Biol. 112*, 665–676]. Binding of domain 2 to actin filaments was Ca^{2+}-dependent and saturated at a 1:1 molar ratio. In the presence of Ca^{2+}, about 1.5 mol of domains 2+3 bound per mole of F-actin subunit. Scatchard analysis gave a K_d of 18 μM for the interaction of domain 2 with F-actin subunits and a K_d of 1.6 μM for domains 2+3. Low-shear viscometry, electron microscopy, and low-speed sedimentation assays showed that domains 2+3 induced bundling of actin filaments. The influence of PIP_2 micelles on the different activities of severin was assayed using native severin and N- and C-terminally truncated fragments. Severin contains at least two PIP_2-binding sites since the activities of the two nonoverlapping severin fragments domain 1 and domains 2+3 were inhibited by PIP_2. The specificity of severin–phospholipid interaction was investigated by studying the regulation of native severin by PIP_2 and other pure or mixed phospholipids. Severin was inhibited not only by PIP_2 and PIP micelles but also by other negatively charged phospholipids such as PI and PS. This result is in contrast to data previously obtained with gelsolin and villin, but in agreement with findings on adseverin from bovine adrenal medulla. However, the specificity for PIP_2 was increased when the pH was lowered from 8.1 to 6.6. Under all conditions tested, IP_3 and neutral phospholipids such as PC and PE did not affect the severing activity. We conclude that severin contains one actin-binding site in each domain, namely, a capping site in domain 1 and two F-actin side-binding regions in domains 2+3. Two distinct Ca^{2+}-binding activities are associated with domains 1 and 2 and two PIP_2-binding regions are present, one in domain 1 and the other in domains 2+3.

A large number of actin-binding proteins are engaged in the regulation of the microfilament system in nonmuscle cells [for reviews, see Stossel et al. (1985), Pollard and Cooper (1986), and Vandekerckhove (1990)]. The Ca^{2+}-activated and PIP_2-inhibited[1] F-actin-fragmenting proteins are thought to regulate actin filament length upon agonist stimulation via their F-actin fragmenting and capping activities. A prerequisite for fast and directed elongation of actin filaments is the availability of free barbed ends together with a release of actin monomers. This might be done by elevated levels of polyphosphoinositides which lead to removal of capping proteins from barbed ends (Stossel, 1989).

Severin from *Dictyostelium discoideum* (Brown et al., 1982), fragmin from *Physarum polycephalum* (Hasegawa et al., 1980), the vertebrate proteins gelsolin (Yin & Stossel, 1979), villin (Bretscher & Weber, 1979), and adseverin, also called scinderin (Maekawa et al., 1989; Del Castillo et al., 1990), belong to the group of actin-filament-fragmenting proteins which are composed of highly conserved domains (Kwiatkowski et al., 1986; Ampe & Vandekerckhove, 1987; Andrē et al., 1988; Arpin et al., 1988; Schleicher et al., 1988; Sakurai et al., 1991). Severing is thought to be a sequential interaction of distinct binding sites between the actin-binding protein and the actin filament (Matsudaira & Janmey, 1988). To elucidate the domain structure of *Dictyostelium* severin, C-terminally deleted fragments were expressed in *Escherichia coli*, purified to homogeneity, and then characterized in functional assays (Eichinger et al., 1991). Domain 1 harbored the actin filament capping but not the fragmenting activity, due to the lack of an F-actin side-binding region.

Here we describe studies with severin fragments consisting either of domain 1 (DS151), domain 2 (DS111M), or the tandem domains 2+3 (DS211C). In addition, we characterized the interaction of severin and its fragments with PIP_2 and other phospholipids. The results show that severin contains three actin-binding sites and at least two Ca^{2+}- and two PIP_2-binding sites. The severing, capping, monomer-binding, and F-actin side-binding activities of severin and its fragments could be inhibited by PIP_2. This inhibition was not strictly specific since all negatively charged phospholipids tested were active to some extent. Neutral phospholipids and IP_3 did not inhibit the severing activity. Similarly, the severing and nucleating activities of adseverin are inhibited not only by polyphosphoinositides but also by other acidic phospholipids (Maekawa & Sakai, 1990), whereas the interaction of gelsolin

† This work was supported by the Grant Schl204/2 from the Deutsche Forschungsgemeinschaft. L.E. is a recipient of a fellowship from the Max-Planck Society.

* Correspondence should be sent to this author at the Max-Planck-Institut für Biochemie, Am Klopferspitz 18a, 8033 Martinsried, Federal Republic of Germany.

[1] Abbreviations: DEAE, (diethylamino)ethyl cellulose; EGTA, ethylene glycol bis(β-aminoethyl ether)-*N*,*N*'-tetraacetic acid; IP_3, inositol trisphosphate; IPTG, isopropyl β-D-thiogalactopyranoside; PC, phosphatidylcholine; PE, phosphatidylethanolamine; PI, phosphatidylinositol; PIP, phosphatidylinositol 4-monophosphate; PIP_2, phosphatidylinositol 4,5-bisphosphate; PMSF, phenylmethanesulfonyl fluoride; PS, phosphatidyl-L-serine; SDS–PAGE, sodium dodecyl sulfate–polyacrylamide gel electrophoresis.

0006-2960/92/0431-4779$03.00/0

with phospholipids has been reported to be specific for PIP_2 and PIP (Janmey & Stossel, 1987, 1989). With respect to its interaction with phospholipids, severin therefore seems to be closer related to adseverin than to gelsolin.

Materials and Methods

Construction, Expression, and Purification of Severin and Truncated Severin Molecules. cDS636 and cDS336 coding for DS211C (domains 2+3) and DS111M (domain 2), respectively, were constructed by polymerase chain reaction (PCR) using cDS4, a cDNA coding for complete severin of *D. discoideum*, as a template (Andrê et al., 1989). The severin fragments are designated according to the number of amino acids as DS151 (amino acids 1–151 of *Dictyostelium* severin), DS111M (amino acids 152–262, representing the middle domain), and DS211C (amino acids 152–362, representing the C-terminal two domains). Primers 1 and 2 were used for the construction of cDS636 and primers 1 and 3 for the construction of cDS336. Primer 1 (34-mer; 5′-CGCG AAT TCC AAT CAT GTT AAA CCA ACA GAA TAT-3′) was specific for bases coding for the N-terminus of domain 2 of *D. discoideum* severin, primer 2 (35-mer, 5′-GCG GAA TTC **TTA** AGC AGA TAA TAA AGT TTC AAA TG-3′) was specific for the 3′-end of the severin cDNA upstream of the TAA stop codon, and primer 3 (34-mer, 5′-CGC GAA TCC **TTA** GGC AGT TTC GTG TTT AGC AGC G-3′) was specific for bases coding for the C-terminus of domain 2. The *Eco*RI restriction sites of the 5′ "add-on" sequences (Scharf et al., 1986) are underlined, and the TAA stop codons of primer 2 and 3 are printed in bold. The PCR reaction and the cloning of the PCR product were performed as described (Eichinger et al., 1991). Due to construction and cloning into the *Eco*RI site of pIMS1 (Simon et al., 1988) DS211C and DS111M each contained three additional amino acids (M-N-S) at the N-terminus.

For expression of DS211C and DS111M, recombinant *E. coli* JM83 cells were grown at 37 °C to an OD_{580} of 0.5, induced with 0.5 mM IPTG, and further incubated for 2 h at 37 °C. The cells were harvested by low-speed centrifugation (4000*g*, 10 min), washed once with 1 mM Tris-HCl, pH 8.0, 1 mM ethylenediaminetetraacetic acid (EDTA), resuspended in a small volume (15 mL/L of recombinant JM83) of TEDABP buffer (10 mM Tris-HCl, pH 7.2, 1 mM EGTA, 1 mM DTT, 0.02% NaN_3, 1 mM benzamidine, 0.5 mM PMSF), and opened by ultrasonication. Insoluble material was pelleted (20 min, 30000*g*), and proteins were further extracted from the pellet in a Dounce homogenizer with TEDABP buffer containing 30% sucrose. After centrifugation (20 min, 30000*g*) this procedure was repeated with TEDABP buffer and 2 M urea, and then three times with TEDABP buffer containing 6 M urea; and for analytical purposes, the final pellet was resuspended in 1% SDS and 1 mM β-mercaptoethanol and incubated for 3 min in a boiling water bath. SDS–PAGE of aliquots of the supernatants showed that most of the DS211C was extracted with TEDABP buffer containing 6 M urea and only a minor amount was extracted with 2 M urea and with 1% SDS. The extracts with 6 M urea containing DS211C were pooled, dialyzed versus the same buffer with 5 M urea, and subjected to anion-exchange chromatography (DE52, 2.5 × 6 cm, equilibrated in the same buffer). Under the conditions used, DS211C did not bind to the resin. The flow-through was collected, precipitated with ammonium sulfate (70% saturation), and centrifuged (20000*g*, 20 min). The pellet was dissolved in TEDABP buffer containing 6 M urea, dialyzed in several steps against TEDABP buffer containing 200 mM NaCl, and then gel filtered on Sephacryl S300 (2.5 × 100 cm) using the same buffer. DS211C containing fractions were pooled, dialyzed against buffer A (2 mM Tris-HCl, pH 7.6, 0.2 mM Na_2ATP, 0.2 mM $CaCl_2$, 0.5 mM DTT, 0.01% NaN_3), concentrated with Amicon concentrator tubes, and stored in aliquots at −70 °C.

Most of the DS111M was found in the soluble fraction after opening the cells by ultrasonication. In analytical experiments, the remaining part of DS111M could be extracted with TEDABP buffer containing 30% sucrose and with the same buffer containing 2 M urea. For further purification of DS111M, the soluble fraction was subjected to anion-exchange chromatography (DE52, 2.5 × 6 cm, equilibrated in TEDABP buffer, pH 7.2). The flow-through was collected, dialyzed versus MEDABP buffer (10 mM MES pH 6.5, 1 mM EGTA, 1 mM DTT, 0.02% NaN_3, 1 mM benzamidine, 0.5 mM PMSF), and then loaded onto a phosphocellulose column (P11, 2.5 × 6 cm, equilibrated in the same buffer). Most contaminating proteins remained in the flow-through; bound DS111M was step-eluted with 400 mM NaCl and size fractionated in TEDANBP buffer (TEDABP buffer plus 200 mM NaCl) using an S300 column (4 × 88 cm). Pure DS111M was pooled, dialyzed versus buffer A, concentrated with Amicon concentrator tubes, and stored in aliquots at −70 °C. From 1 L of induced *E. coli* cells about 5 mg of DS211C and about 40 mg of DS111M were purified. Construction, expression, and purification of severin, DS277, DS177 (amino acids 1–277 and 1–177 of *Dictyostelium* severin), and DS151 have been described elsewhere (Eichinger et al., 1991).

Sedimentation Assays. The finding that F-actin could be sedimented in the presence of DS211C in low-speed centrifugations indicated bundling of filaments similar to data obtained by Meyer and Aebi (1990) with the F-actin cross-linking protein α-actinin. Therefore, binding of DS211C to the sides of actin filaments was assayed by high- (120000*g*) and low- (15000*g*) speed centrifugation at 4 °C.

After removal of debris in the G-actin, DS211C, and DS111M solutions by centrifugation for 1 h at 120000*g* in an airfuge (Beckman Instruments), 5 μM G-actin or in the case of DS111M 6 μM G-actin in buffer A was polymerized by the addition of 2 mM $MgCl_2$ in the presence of different concentrations of actin-binding protein. The influence of Ca^{2+} was tested by adding 1 mM EGTA to buffer A. To mimic physiological conditions better than can be done by KCl, we used potassium glutamate (100 mM) for higher stringency. Cosedimentation was tested at molar ratios ranging from 30:1 to 1:3 (actin to DS211C) and from 5:1 to 1:8 (actin to DS111M). Molar ratios for analysis of binding constants according to Scatchard (1949) were as follows: actin to DS211C, 3:1, 2:1, 1.75:1, 1.5:1, 1.25:1, 1:1, 1:1.25, 1:1.5, 1:1.75, 1:2, 1:2.5, and 1:3; actin to DS111M, 3:1, 2:1, 1.5:1, 1:1, 1:1.25, 1:1.5, 1:1.75, 1:2, 1:2.5, 1:3, 1:4, and 1:5. Apparent dissociation constants were calculated according to the Scatchard equation:

$$B/F = (n - B)/K$$

where B is moles of severin fragment bound per mole of actin, F is the amount of free severin fragment in moles, n is the total number of binding sites, and K is the dissociation constant. After 2 h at room temperature, 80-μL samples were centrifuged as above in the airfuge. With DS211C, the sedimentation of actin was tested also in low-speed centrifugations (15000x*g*, 30 min) at molar ratios indicated in Figure 2C. The pellets were solubilized in the original volume, and the distribution of actin and DS211C in pellets and supernatants was judged by SDS–PAGE (15% acrylamide) and Coomassie blue staining. To quantify the cosedimentation of DS211C and

DS111M with actin, the protein bands were scanned (Elscript 400, Hirschmann Co., FRG) and calculated relative to cosedimented actin.

Electron Microscopy. G-actin and DS211C solutions were precentrifuged at 120000*g* for 30 min at 4 °C. After polymerization of 60 μM G-actin in buffer A with 2 mM $MgCl_2$ for 30 min, the actin filaments were diluted to 10 μM and incubated with different concentrations of DS211C (molar ratios of DS211C to actin: 1:8, 1:4, 1:2, 1:1, 0:1) for 30 min. For comparison, paracrystal formation of 50 μM F-actin was induced by incubation with 20 mM $MgCl_2$ for 1 h. The samples were then applied to formvar-coated copper grids (400 mesh) which had been layered with carbon, stained with an aqueous solution of 2% uranyl acetate, examined, and photographed in a microscope (100CX; JEOL USA, Analytical Instruments Division, Cranford, NJ) at 80 kV with a magnification of 33 000.

Low-Shear Viscometry. Low-shear viscometry with DS211C or DS111M was carried out as described (Eichinger et al., 1991). The inhibition of the bundling activity of DS211C by PIP_2 micelles was investigated at a molar ratio of 20:1 (actin to DS211C). First PIP_2, then G-actin, was added to the DS211C-containing solutions, the actin was polymerized, and after 20 min at 25 °C the relative viscosities of the solutions were determined.

Preparation of Phospholipids. Phospholipids that were obtained as lyophilized salts (PIP_2, PIP, and PS) were dissolved in 10 mM Tris-HCl, pH 8.0. The other phospholipids (PI, PC, and PE) that were supplied as chloroform solutions were dried in a stream of nitrogen and then dissolved in 10 mM Tris-HCl, pH 8.0. Single phospholipids and IP_3 were dissolved at a concentration of 1 mM, mixed phospholipids at concentrations between 2 and 7 mM. For the preparation of mixed lipid vesicles, the corresponding phospholipids were combined as salt or chloroform solution at the appropriate molar ratios (PC/PE and PC/PS = 1:1; PC/PE/PS and PC/PE/PIP_2 = 4:2:1). Single or mixed phospholipids were sonicated using a Branson S75 sonicator (Branson Sonic Power Co., Danbury, CT) operating at maximum intensity until an optically clear solution was formed. In the case of a mixture of PC, PE, and PS, the solution remained slightly turbid under all conditions of sonication. Either the phospholipids were used the same day after sonication or they were stored in aliquots at −70 °C. After thawing, stored phospholipids were sonicated in a water bath sonicator for 30–60 min at room temperature and used the same day.

Fluorescence Spectroscopy. Labeling of actin with *N*-(1-pyrenyl)iodoacetamide (pyrene) (Cooper et al., 1983), measurements of the severing activity by dilution-induced depolymerization of F-actin, and assays of G-actin-binding activity by fluorescence enhancement of pyrene-labeled G-actin were essentially performed as described (Eichinger et al., 1991). For kinetic measurements, the excitation wavelength was 365 nm and the emission wavelength was 386 nm with the exception of measurements with mixed phospholipid vesicles where the emission wavelength was set to 407 nm to avoid interfering light scattering. Care was taken to minimize aggregation of phospholipid micelles or vesicles.

Capping of Actin Filaments. The ability of DS151 (domain 1 of severin) to bind to the (+) end of actin filaments and the inhibition of this capping activity by PIP_2 micelles was tested by following the depolymerization kinetics of pyrene-labeled F-actin which was diluted below the critical concentration of the barbed end. Proteins that bind to the barbed end of the filament can retard the rate of depolymerization nearly 10-fold (Walsh et al., 1984). Pyrene-labeled F-actin (8 μM) in buffer B were diluted to 80 nM into solutions containing increasing concentrations of either DS151 or PIP_2 micelles, with or without a constant concentration of 160 nM DS151. PIP_2 micelles alone did not change the depolymerization kinetics of pyrene-labeled F-actin. The difference between the fluorescence decrease per minute of the control (depolymerization rate of 80 nM pyrene-labeled F-actin without any additional protein) and the fluorescence decrease per minute in the presence of 160 nM DS151 was defined as 100% capping activity. Usually from three experiments, the mean values of the fluorescence decrease per minute in the linear range were calculated and then expressed as relative capping activity. Changes in tryptophan fluorescence were exploited for monitoring binding of Ca^{2+} to DS211C and DS111M. The assay was performed as described (Eichinger et al., 1991).

Miscellaneous. Actin was prepared from rabbit skeletal muscle (Spudich & Watt, 1971) and gel filtered on Sephacryl S300. The concentration of actin and pyrene-labeled actin was measured as described (Cooper et al., 1983). All other protein concentrations were determined by the method of Bradford (1976) using BSA as a standard. SDS–PAGE was done on minislab gels (110 × 83 × 0.5 mm) using the buffer system of Laemmli (1970). The marker proteins for calibrating the Superose 12 gel filtration column and Sephacryl S300 were purchased from Pharmacia (Uppsala, Sweden), DEAE-cellulose (DE52) from Whatman (Maidstone, England), phospholipids and IP_3 from Sigma (Deisenhofen, FRG), and *N*-(1-pyrenyl)iodoacetamide from Molecular Probes (Pitchford, OR). All chemicals were of analytical grade.

Results

Purification and Characterization of DS211C and DS111M. An overview of the domain structure of severin deduced from sequence comparisons to gelsolin, villin, and fragmin (Way & Weeds, 1988), the complete severin cDNA clone cDS4 with the cis-active elements of pIMS1 (Simon et al., 1988), and the relative sizes of whole severin, domain 1 (DS151), domain 2 (DS111M), and the tandem domains 2+3 (DS211C) are shown in Figure 1A. For purification of DS211C, treatment with 6 M urea was needed to solubilize the protein from inclusion bodies. To exclude oligomers of DS211C which could have been formed during renaturation, we performed gel filtration under native conditions as the last purification step. The pool of purified DS211C was analyzed on a sizing column, and it could be shown that the DS211C (23 700 Da) pool consisted exclusively of monomers (data not shown). In contrast to DS211C, DS111M (12 300 Da) was found in the soluble fraction after opening the cells by ultrasonication. In Figure 1B essential purification steps of DS211C and DS111M from *E. coli* homogenate to pure protein are shown. To assay for minor contaminations, the proteins from highly concentrated samples were analyzed by SDS–PAGE and showed a purity of more than 99%. During the purification of DS211C a degradation product of approximately 22 000 Da was detectable and could not be separated from the entire DS211C polypeptide. The amount of degradation product never exceeded a level of approximately 10%, and in sedimentation assays it behaved like the complete DS211C. Sequencing of the N-terminus by Edman degradation showed no change in the amino acid sequence, thus indicating that a small part of the C-terminus had been cleaved off.

The binding of DS211C and DS111M to actin filaments was investigated by high-speed centrifugations in the presence or absence of Ca^{2+}. To determine the stoichiometry and

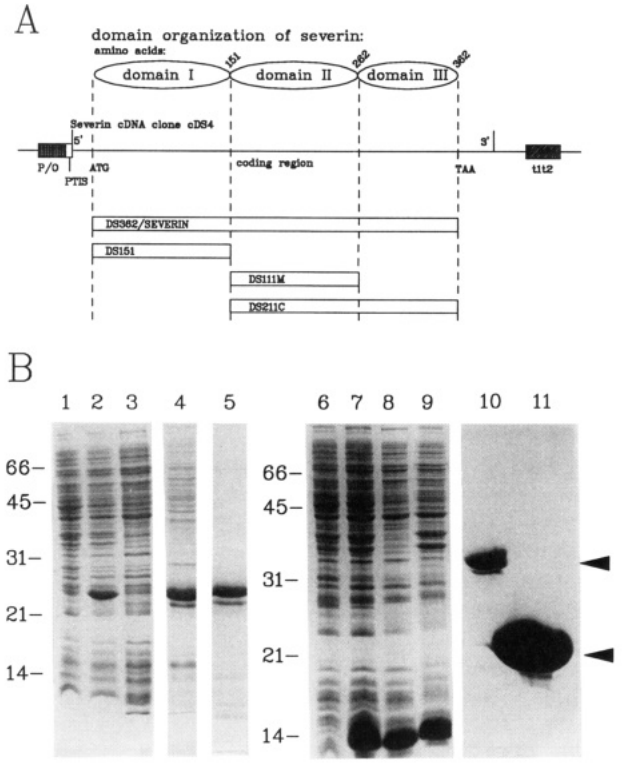

FIGURE 1: (A) Schematic presentation of the complete severin clone cDS4, the relative sizes of severin derivatives characterized (open bars), and the domain organization of *Dictyostelium* severin deduced from sequence comparisons with gelsolin, villin, and fragmin. The 5′- and 3′-ends and the start and stop codons of the severin cDNA and the cis-active elements of the pIMS1 expression vector are shown (P/O, tac promoter and operator; PTIS, portable translation initiation site; t1t2, transcriptional terminators). (B) SDS–PAGE (15% acrylamide) and Coomassie blue staining of DS211C (lanes 1–5 and 10) and DS111M (lanes 6–9 and 11) at different stages of purification. (Lanes 1 and 6) Total *E. coli* cell homogenates; (lanes 2 and 7) total cell homogenates of *E. coli* cells induced with 0.5 mM IPTG; (lanes 3 and 8) supernatants after opening the cells; (lane 4) supernatant after extraction with 6M urea; (lane 5) flow-through of the DE52 column; (lane 9) supernatant after extraction with 30% sucrose; (lanes 10 and 11) overloading with purified DS211C (6 μg) and DS111M (120 μg). The sizes of the molecular mass markers in kilodaltons are shown on the left of each panel.

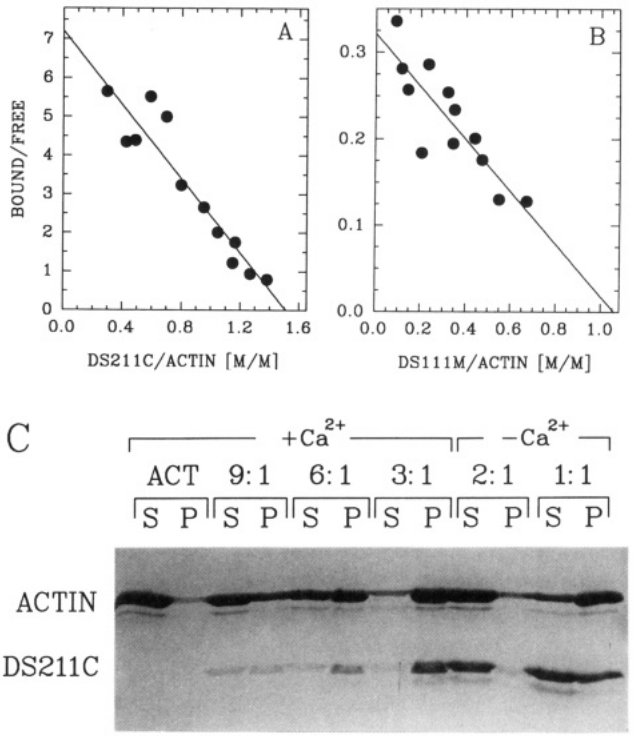

FIGURE 2: Scatchard plots of DS211C (A) and DS111M (B). Different molar ratios of G-actin to DS211C (from 3:1 to 1:3) or to DS111M (from 3:1 to 1:5) were copolymerized, centrifuged at 120000*g*, the pellets solubilized in the original volume, and the proteins from the supernatants and pellets subjected to SDS–PAGE. The Coomassie blue stained gels were scanned, and the amounts of DS211C and DS111M in supernatants ("free") and pellets ("bound") were calculated and plotted versus bound protein per actin. (C) Low-speed sedimentation of F-actin in the presence of DS211C. Different molar ratios of G-actin to DS211C (indicated above the figure) were copolymerized either in the presence or absence of Ca^{2+}, centrifuged at 15000*g* for 30 min, and the supernatants (S) and pellets (P) analyzed by SDS–PAGE.

apparent affinity of the interaction of DS211C and DS111M with F-actin subunits under high-stringency conditions, binding was measured at varying molar ratios of actin to DS211C or DS111M by densitometric analysis of supernatants and pellets of Coomassie blue stained SDS–polyacrylamide gels and then analyzed using the method of Scatchard (1949). Binding of DS211C to actin was saturable with a binding capacity of about 1.5 mol of DS211C per mole of actin and an apparent dissociation constant (K_d) of 1.6 μM in the presence of Ca^{2+} (Figure 2A). This value was obtained if one assumed two independent actin-binding sites in DS211C. The binding was drastically reduced in the presence of EGTA. Binding of DS111M to actin was saturable with a binding capacity of about 1.05 mol of DS111M per mole of actin and an apparent K_d of 18 μM in the presence of Ca^{2+} (Figure 2B). Saturation at a 1:1 molar ratio suggests binding of one DS111M molecule per actin subunit in the filament. In the presence of EGTA, only minimal quantities of DS111M were observed together with F-actin in the pellet fraction. The data indicate that both side-binding polypeptides are Ca^{2+}-regulated; consistently, both proteins changed their tryptophan fluorescence after addition of Ca^{2+} (data not shown). The K_d of 1.6 μM in DS211C represents the product of the two separate dissociation constants for the binding of domain 2 and of domain 3 to actin. In a first approximation, a K_d of about 0.1 μM could then be calculated for the binding of domain 3 to actin subunits in the filament. Binding of DS211C to F-actin was also investigated at low-speed centrifugations. As shown in Figure 2C, addition of DS211C to actin rendered the polymerized actin pelletable at 15000*g*. In the presence of Ca^{2+}, an increase in the pellet fraction of F-actin was already found at a molar ratio of 9 actin to 1 DS211C, and nearly complete sedimentation was found at a molar ratio of 3:1. Actin alone remained in the supernatant. In the absence of Ca^{2+} a 1:1 molar ratio of actin to DS211C was necessary to sediment most of the actin, reflecting again a considerably decreased affinity of DS211C to actin in EGTA. This result suggests that DS211C might contain two F-actin binding sites which are exposed after removal of domain 1 and are able to induce bundling of actin filaments. In agreement with the data from the sedimentation assays, we found that in the presence of Ca^{2+} the viscosity of an F-actin solution was strongly increased after addition of DS211C, while in the absence of Ca^{2+} even high concentrations of this severin mutant increased the viscosity only weakly. Even high concentrations of DS111M (up to molar ratios of DS111M to actin of 2:1) did not influence the viscosity of the F-actin solution either in the presence or in the absence of Ca^{2+} (Figure 3A). This result also renders a G-actin-binding activity of DS111M as very unlikely because removal of G-actin from the polymerization equilibrium should lower the viscosity. Fluorescence enhancement of pyrene-labeled G-actin was exploited to compare binding of severin, DS151, DS211C, and DS111M to G-actin. Figure 3B shows that, at equimolar

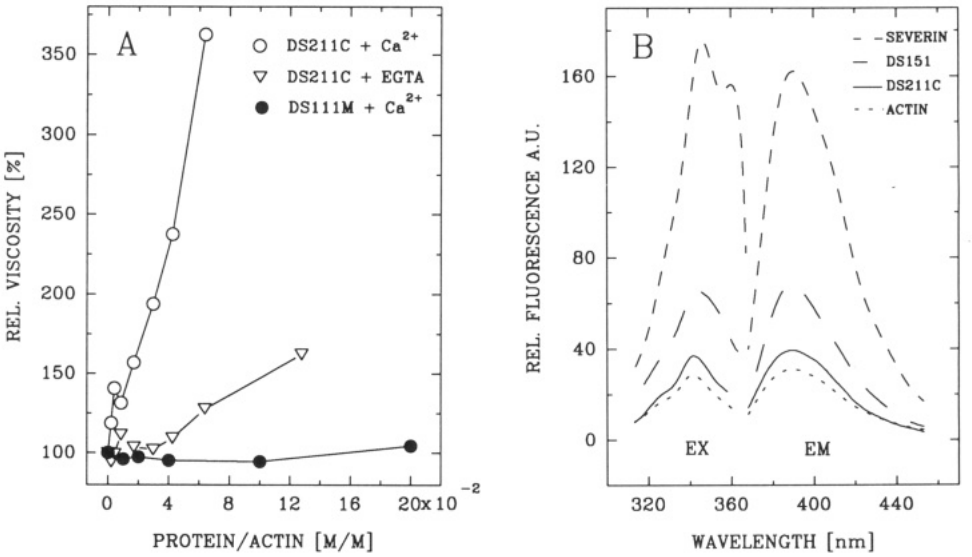

FIGURE 3: (A) Low-shear viscometry with increasing concentrations of DS211C and DS111M in the presence or absence of 0.2 mM Ca^{2+}. (B) Fluorescence enhancement in arbitrary units (A.U.) of pyrene-labeled G-actin (short dashed line) upon binding of DS211C (solid line), DS151 (long dashed line), or severin (medium dashed line) in the presence of Ca^{2+}. The excitation scans (EX) or emission scans (EM) were corrected either for the buffer fluorescence or for the fluorescence of the buffer plus the corresponding protein. The excitation spectra were recorded at the emission wavelength of 386 nm and the emission spectra with excitation at 343 nm; all proteins had a concentration of 200 nM.

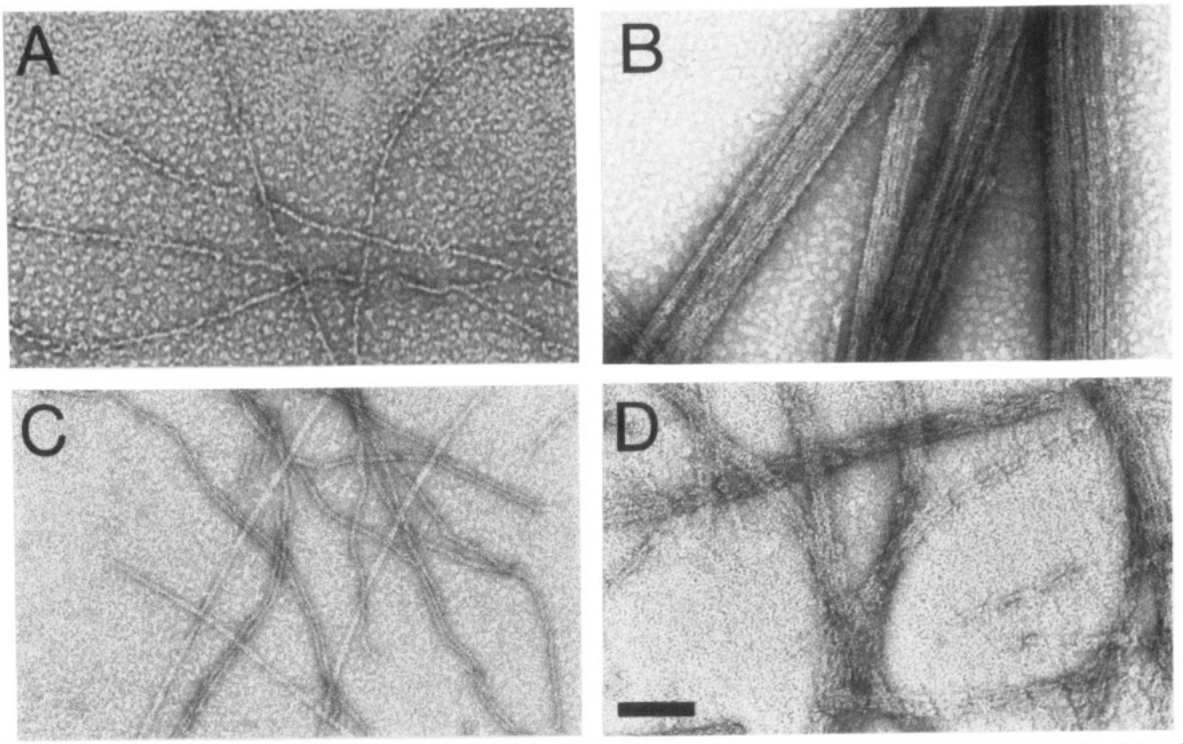

FIGURE 4: Electron microscopy of negatively stained (2% uranyl acetate) actin filaments (A), paracrystals of actin filaments induced by addition of 20 mM Mg^{2+} (B), and bundles of actin filaments induced by addition of DS211C (C and D). The molar ratios of actin to DS211C were 8:1 (C) and 1:1 (D). The bar represents 100 nm.

ratios, the fluoresence of pyrene-labeled G-actin in excitation as well as emission scans was drastically increased by severin while only a moderate increase was observed with DS151 and DS211C. No fluorescence enhancement was detectable with DS111M (data not shown).

In addition, we investigated the mode of interaction between DS211C and F-actin by electron microscopy. Figure 4 shows micrographs of negatively stained actin filaments alone (Figure 4A) and Mg^{2+}-induced paracrystals of F-actin (Figure 4B) in comparison to filaments which were mixed after polymerization with different amounts of DS211C (Figure 4C,D). Also from these studies, it is obvious that DS211C caused bundling of actin filaments in a concentration-dependent manner.

Regulation of Severin and Severin Fragments by Phospholipids. Recently, it was shown that the filament-fragmenting activity of severin can be directly inhibited by PIP_2 (Yin et al., 1990). To identify distinct PIP_2-binding regions in the severin molecule, we used bacterially expressed severin fragments described in this report and in addition constructs that lacked from the C-terminal end 85 (DS277) and 185 (DS177) amino acids (Eichinger et al., 1991). Figure 5A shows that the severing activity of severin and the two C-terminally truncated fragments DS277 and DS177 was in-

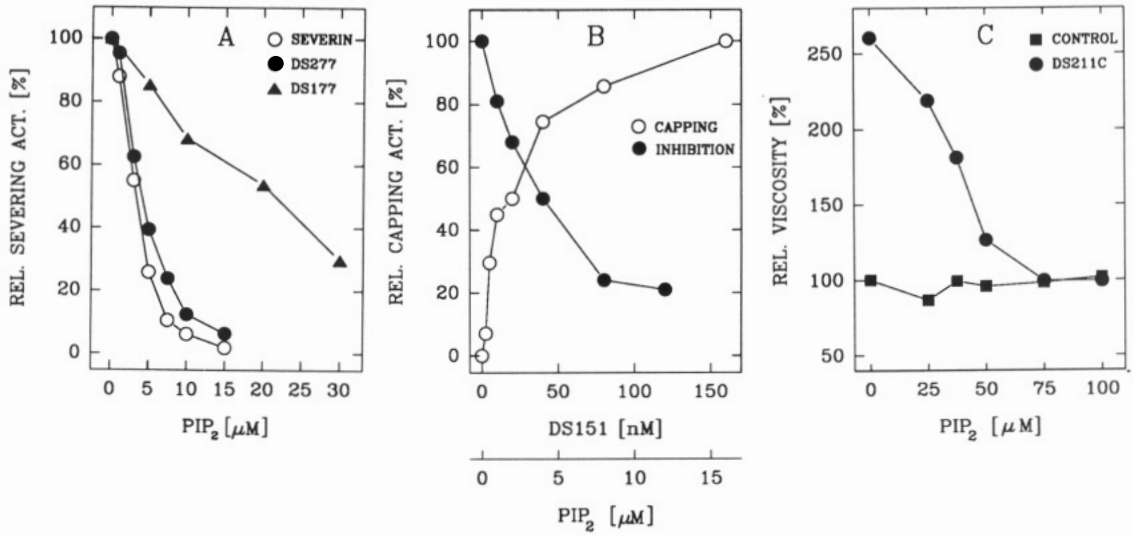

FIGURE 5: Inhibition of the severing (A), capping (B), and bundling (C) activity of severin or severin fragments by PIP_2. (A) Inhibition of the filament fragmenting activity of native severin (25 nM) and the bacterially expressed severin derivatives DS277 (40 nM) and DS177 (400 nM) in dilution-induced depolymerization assays with increasing concentrations of PIP_2. (B) Capping activity of DS151, the first domain of severin, and its inhibition by PIP_2. The influence of increasing concentrations of DS151 on the depolymerization rate of 80 nM pyrene-labeled F-actin was compared to the depolymerization rate of F-actin alone and calculated as relative capping activity. The capping activity of 160 nM DS151 was defined as 100% and the influence of increasing concentrations of PIP_2 determined. (C) Influence of PIP_2 on the viscosity increasing activity of a fixed DS211C concentration (actin to DS211C ratio, 20:1). PIP_2 had no effect on the viscosity of an F-actin solution without additional protein.

hibited by PIP_2 micelles. Although considerably higher concentrations of PIP_2 had to be used to inhibit the severing activity of DS177, half-maximal inhibition of all three proteins was reached at a molar ratio of 60 to 100 molecules of PIP_2 to one molecule of severing protein. The comparatively high PIP_2 concentration required for the inhibition of DS177 was due to the fact that DS177 is a very weak severing protein, and a 10-fold higher concentration had to be used in this assay. The results clearly showed that a severin fragment containing only the first 177 amino acids of intact severin can be inhibited by PIP_2 micelles. To further elucidate the site(s) responsible for PIP_2 regulation, we investigated the influence of PIP_2 micelles on the capping activity of domain 1 (DS151) and on the viscosity increasing activity of the tandem domains 2+3 (DS211C). Using the dilution-induced depolymerization assay, we defined the maximal decrease in the depolymerization rate of F-actin in the presence of 160 nM DS151 (Figure 5B, capping) as 100% capping activity. Increasing concentrations of PIP_2 micelles, preincubated for about 1 min with DS151, caused a decrease in the relative capping activity of DS151, and at a molar ratio of about 30 PIP_2 molecules to one molecule of DS151 half-maximal inhibition was observed (Figure 5B, inhibition). Surprisingly, not only the capping activity of DS151 but also the viscosity increasing activity of the tandem domains 2+3 (DS211C) was sensitive to PIP_2 micelles. Figure 5C shows that PIP_2 micelles inhibited the bundling activity of DS211C but had no effect on the relative viscosity of F-actin alone. Half-maximal inhibition of the bundling activity of DS211C was reached at a molar ratio of about 80 PIP_2 molecules to one molecule of DS211C.

Binding of severin to G-actin and its regulation by EGTA and PIP_2 micelles was assayed under nonpolymerizing conditions with 200 nM pyrene-labeled G-actin. In the presence of Ca^{2+}, maximal fluorescence enhancement was observed at a molar ratio of approximately 1.3:2 (severin to actin) which indicated binding of two actin molecules to one severin molecule. Higher concentrations of severin resulted in lower fluorescence values and at a molar ratio of 1.3 severin to 1 actin a stable level was reached. This showed that excess severin competed with a high-affinity site for the second bound

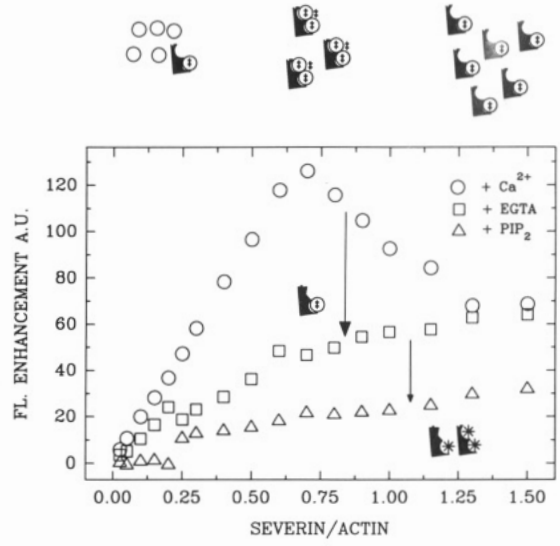

FIGURE 6: G-actin-binding activity of severin and inhibition by subsequent addition of EGTA and PIP_2. The fluorescence enhancement in arbitrary units (A.U.) of 200 nM pyrene-labeled G-actin upon binding to severin under nonpolymerizing conditions is plotted versus the molar ratio of severin to actin in the presence of Ca^{2+}, after addition of EGTA, and after further addition of PIP_2. The schematic drawings above the plot show the complexes which could be formed at changing severin to actin ratios in the presence of Ca^{2+}. Symbols inside the plot indicate from top to bottom release of one actin from the 1:2 complex by addition of EGTA and further release of the actin in the EGTA stable 1:1 complex by addition of PIP_2. PIP_2 was also found capable to release both actins bound to severin in the 1:2 complex (symbol in the lower right). The double crosses represent emitted fluorescence upon binding of pyrene-labeled G-actin to severin. We suggest that the synergistic increase of fluorescence in the trimeric complex is based on the formation of an F-actin dimer.

actin from the severin/$actin_2$ complex leading to a stable heterodimer (Figure 6, open circles). Addition of EGTA to trimeric severin/actin complexes preformed in Ca^{2+} caused a significant fluorescence decrease, indicating that 1:1 heterodimers remained (Figure 6, open squares). The binding data in the presence of EGTA were analyzed using Scatchard plots, and a K_d of about 2 nM was calculated for the binding

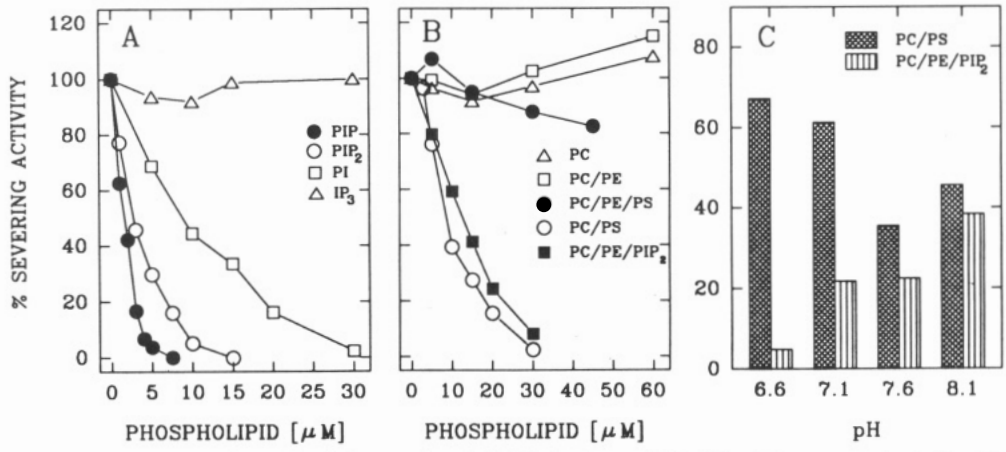

FIGURE 7: Specificity of the interaction of severin with pure phospholipid micelles and IP_3 (A), with pure or mixed phospholipid vesicles (B), and influence of different pH values on the inhibitory effect of PC/PS and PC/PE/PIP_2 vesicles (C). (A) The severing activity of 50 nM severin was determined by dilution-induced depolymerization of F-actin, defined as 100%, and the influence of increasing concentrations of PIP, PIP_2, PI, or IP_3 on this severing activity was investigated. (B) The influence of increasing concentrations of PC, PC/PE (molar ratio of 1:1), PC/PE/PS (molar ratio of 4:2:1), PC/PS (molar ratio of 1:1), or PC/PE/PIP_2 (molar ratio of 4:2:1) on the severing activity of 25 nM severin is shown. The values on the *X*-axis (micromolar phospholipid) correspond to the last-mentioned phospholipid in the mixture. (C) Comparison of the inhibitory effect of PC/PS (molar ratio of 1:1, 30 μM PS) and PC/PE/PIP_2 (molar ratio of 4:2:1, 20 μM PIP_2) on the severing activity of 20 nM severin at different pH values. The severing activity of 20 nM severin in the absence of phospholipid at each pH value was defined as 100%.

of severin to G-actin after addition of EGTA (data not shown). This is in very good agreement with reported K_d values between 0.1 and 25 nM in the presence of Ca^{2+} (Giffard et al., 1984). Addition of PIP_2 micelles to the EGTA-resistant 1:1 complex resulted in a further fluorescence decrease, indicating that the actin bound in the 1:1 complex could be released by PIP_2 (Figure 6, open triangles). Addition of PIP_2 micelles to the trimeric complex in the presence of Ca^{2+} decreased the fluorescence down to the lowest level (data not shown). This suggests that both actin molecules bound in the trimeric complex can be released by PIP_2.

Inhibition of the filament-fragmenting activity of native *Dictyostelium* severin was used to study the specificity of single and mixed phospholipids. Highest inhibition was observed with PIP and PIP_2. PI micelles were able to inhibit the severing activity at higher concentrations than PIP or PIP_2 micelles while IP_3 even at high concentrations did not influence the severing activity (Figure 7A). PC and PC/PE vesicles had no inhibitory effect on the severing activity, and mixed phospholipid vesicles composed of the three components PC, PE, and PS slightly inhibited the severing activity by about 20% only at high concentrations. Surprisingly, vesicles composed of PC and PS were as efficient in inhibiting the severing activity as vesicles composed of PC/PE/PIP_2. However, in comparing the inhibitory effect of PC/PE/PS and PC/PE/PIP_2 vesicles, PIP_2 turned out to be a far better inhibitor of the severing activity of severin than PS in an identical phospholipid environment (Figure 7B). It seems obvious that the charge density is of major importance, since PS with its single negative charge was a weak inhibitor if it constituted only a small fraction of the vesicles. Lowering the pH in the severing assay from 8.1 to 6.6 in three steps successively increased the inhibitory effect of mixed vesicles composed of PC/PE/PIP_2, whereas the inhibitory effect of PC/PS vesicles was significantly decreased (Figure 7C). This indicated that inhibition of severing activity in vivo could be mediated by PIP_2, depending on the intracellular pH and the membrane lipid composition.

Discussion

The data in this report indicate that the F-actin fragmenting protein severin contains two lipid-binding, two Ca^{2+}-binding, and three actin-binding sites. Exploiting the domain structure of severin, we studied the in vitro functions of domain 1 (DS151), domain 2 (DS111M), and the tandem domains 2+3 (DS211C). The reason to choose the tandem domains 2+3 and not the single domain 3 was the expected intriguing behavior of this polypeptide due to its putative two F-actin binding sites. Indeed, although the native severin has a viscosity decreasing function based on its severing and capping properties, this distinct part of the molecule contained an intrinsic F-actin cross-linking activity. This enabled us to assay the regulation of its actin-binding activities by using low-shear viscometry, electron microscopy, and low-speed sedimentation and to determine an approximate K_d for binding to actin subunits in the filament.

Low-shear viscometry was an especially sensitive assay to measure cross-linking of actin filaments by DS211C. A clear Ca^{2+}-dependent increase in viscosity was already observed at a molar ratio of 100 actin molecules to 1 DS211C molecule. The strongly reduced ability to cross-link filaments in the absence of Ca^{2+} was furthermore an appropriate control to exclude the influence of incorrect refolding after protein purification and of nonspecific binding to F-actin due to the rather basic pI of the severin fragment (calcd 8.3). The cross-linking activity could not be the result of DS211C dimer formation. The last purification step was gel filtration chromatography under nondenaturing conditions. Rechromatography on a calibrated sizing column showed that purified DS211C consisted exclusively of monomers. The large actin bundles formed by DS211C were sedimentable at 15000*g* and looked very similar but not identical to Mg^{2+}-induced F-actin paracrystals. The different pattern was probably due to the spacing of filaments by the decorating tandem domains. From Scatchard analysis, we draw the conclusion that most likely the two actin-binding sites of DS211C recognize different target regions on the actin molecule. The tandem domain DS211C had a binding stoichiometry of approximately 1.5 DS211C molecules per F-actin subunit. This suggests two different binding sites for DS211C at the actin molecule which do not compete for each other. Saturation of binding to actin filaments below the expected molar ratio of 2:1 (DS211C/actin) might be due to the cross-linking stoichiometry. Partial steric inhibition of binding of DS211C to actin helices packed

into tight bundles has also to be considered. This interpretation of the Scatchard analysis agrees with data from Pope et al. (1991) which suggest that the two actin-binding sites of the gelsolin domains S2+3 and S4+5+6 interact with distinct regions on the actin molecule. The middle domain DS111M of severin contains only one actin-binding site with a binding stoichiometry of approximately 1 mol of DS111M per mol of actin. Consequently, this domain did neither increase the viscosity of an F-actin solution nor induce the formation of sedimentable actin bundles.

An interesting change of fluorescence was observed during the studies on G-actin binding properties of the severin domains. There was no alteration of the intrinsic fluorescence in pyrene-labeled G-actin after addition of the middle domain DS111M. This argues strongly against an interaction with actin monomers. A significant increase of fluorescence provided evidence for binding of the first domain (DS151) to G-actin. A slight increase of fluorescence was observed with the tandem domains 2+3 (DS211C) under identical conditions. However, the fluorescence increase of labeled G-actin upon binding to complete severin (domains 1–3) was not the sum of the increments found with the isolated domains 1 and 2+3. The dramatic enhancement of fluorescence emission indicates in addition to the binding to severin an interaction of the two bound actin molecules. This may explain how severin nucleates actin polymerization: In a first step domains 1 and 3 bind to individual G-actin molecules and then force the two actin monomers into a dimer configuration, thus shifting the highly unfavored initial steps of actin polymerization by stabilizing the dimer toward elongation. This conformational change would turn two bound actin monomers into two F-actin units with increased fluorescence emission, thus explaining the synergistic effect seen in Figures 3B and 6.

It has been shown recently that the viscosity-decreasing activity of native severin can be inhibited by PIP_2 (Yin et al., 1990). The construction of distinct domains enabled us to study the influence of lipids on the different functions of native severin. Using PIP_2 micelles, we found that the capping activity of domain 1 and the cross-linking activity of the tandem domains 2+3 is inhibited. This result implies the presence of at least two nonoverlapping lipid-binding regions in the whole protein. The specificity of phospholipid interaction with severin was tested using a set of charged and neutral phospholipids. Compared to the high specificity of gelsolin (Janmey & Stossel, 1989) or profilin (Lassing & Lindberg, 1988; Goldschmidt-Clermont et al., 1990) for polyphosphoinositides, severin showed a rather broad specificity for negatively charged phospholipids, similar to adseverin (Maekawa & Sakai, 1990), myosin I (Adams & Pollard, 1989; Hayden et al., 1990), or CapZ (Heiss & Cooper, 1991). However, the interaction of severin with lipids is not simply due to charge differences. The capping activity of domain 1, which has a calculated pI of 6.3, was inhibited by PIP_2 micelles.

It remains to be shown whether the regulation of *Dictyostelium* severin by phospholipids is involved in signal transduction (Dadabey et al., 1991) or an indication for transient distribution of severin along membranes. It should be emphasized that the inhibitory effect of PIP_2 is increased at lower pH values in contrast to PS. Taking the possibility into consideration that slight cytoplasmic pH changes in cAMP-stimulated *Dictyostelium* cells might trigger the interaction of cytoskeletal proteins with microfilaments (Scheel et al., 1988), one might conclude that pH-dependent binding of severin to different populations of cellular lipids is an important regulatory mechanism under in vivo conditions.

ACKNOWLEDGMENTS

We thank Drs. Günther Gerisch, Angelika A. Noegel, and Françoise Veretout for helpful discussions and critical reading of the manuscript, and Hanns-Eugen Stöffler and Ute Zirrgiebel for help in the assays. Electron microscopy of the F-actin paracrystals and bundles would not have been possible without advice by Dr. Murray Stewart.

Registry No. Ca^{2+}, 7440-70-2.

REFERENCES

Adams, R. J., & Pollard, T. D. (1989) *Nature 340*, 565–568.
Ampe, C., & Vandekerckhove, J. (1987) *EMBO J. 6*, 4149–4157.
Andrē, E., Lottspeich, F., Schleicher, M., & Noegel, A. (1988) *J. Biol. Chem. 263*, 722–727.
Andrē, E., Brink, M., Gerisch, G., Isenberg, G., Noegel, A., Schleicher, M., Segall, J. E., & Wallraff, E. (1989) *J. Cell Biol. 108*, 985–995.
Arpin, M., Pringault, E., Finidori, J., Garcia, A., Jeltsch, J.-M., Vandkerckhove, J., & Louvard, D. (1988) *J. Cell Biol. 107*, 1759–1766.
Bradford, M. M. (1976) *Anal. Biochem. 72*, 248–254.
Bretscher, A., & Weber, K. (1979) *Proc. Natl. Acad. Sci. U.S.A. 76*, 2321–2325.
Brown, S. S., Yamamoto, K., & Spudich, J. A. (1982) *J. Cell Biol. 93*, 205–210.
Cooper, J. A., Walker, S. B., & Pollard, T. D. (1983) *J. Muscle Res. Cell Motil. 4*, 253–262.
Dadabay, C. Y., Patton, E., Cooper, J. A., & Pike, L. J. (1991) *J. Cell Biol. 112*, 1151–1156.
Del Castillo, A. R., Lemaire, S., Tchakarov, L., Jeyapragasan, M., Doucet, J.-P., Vitale, M. L., & Trifaro, J.-M. (1990) *EMBO J. 9*, 43–52.
Eichinger, L., Noegel, A. A., & Schleicher, M. (1991) *J. Cell Biol. 112*, 665–676.
Giffard, R. G., Weeds, A. G., & Spudich, J. A. (1984) *J. Cell Biol. 98*, 1796–1803.
Goldschmidt-Clermont, P. J., Machesky, L. M., Baldassare, J. J., & Pollard, T. D. (1990) *Science 247*, 1575–1578.
Hasegawa, T., Takahashi, S., Hayashi, H., & Hatano, S. (1980) *Biochemistry 19*, 2677–2683.
Hayden, S. M., Wolenski, J. S., & Mooseker, M. S. (1990) *J. Cell Biol. 111*, 443–451.
Heiss, S. G., & Cooper, J. A. (1991) *Biochemistry 30*, 8753–8758.
Janmey, P. A., & Stossel, T. P. (1987) *Nature 325*, 362–364.
Janmey, P. A., & Stossel, T. P. (1989) *J. Biol. Chem. 264*, 4825–4831.
Kwiatkowski, D. J., Stossel, T. P., Orkin, S. H., Mole, J. E., Colten, H. R., & Yin, H. L. (1986) *Nature 323*, 455–458.
Laemmli, U. K. (1970) *Nature 227*, 680–685.
Lassing, I., & Lindberg, U. (1988) *J. Cell. Biochem. 37*, 255–267.
Maekawa, S., & Sakai, H. (1990) *J. Biol. Chem. 265*, 10940–10942.
Maekawa, S., Toriyama, M., Hisanaga, S.-I., Yonezawa, N., Endo, S., Hirokawa, N., & Sakai, H. (1989) *J. Biol. Chem. 264*, 7458–7465.
Matsudaira, P., & Janmey, P. (1988) *Cell 54*, 139–140.
Meyer, R. K., & Aebi, U. (1990) *J. Cell Biol. 110*, 2013–2024.
Pollard, T. D., & Cooper, J. A. (1986) *Annu. Rev. Biochem. 55*, 987–1035.
Pope, B., Way, M., & Weeds, A. G. (1991) *FEBS Lett. 280*, 70–74.
Sakurai, T., Kurokawa, H., & Nonomura, Y. (1991) *J. Biol. Chem. 266*, 4581–4585.

Scatchard, G. (1949) *Ann. N.Y. Acad. Sci. 51*, 660–672.
Scharf, S. J., Horn, G. T., & Erlich, H. A. (1986) *Science 233*, 1076–1078.
Scheel, J., Ziegelbauer, K., Kupke, T., Humbel, B., Noegel, A. A., Gerisch, G., & Schleicher, M. (1989) *J. Biol. Chem. 264*, 2832–2839.
Schleicher, M., Andrē, E., Hartmann, H., & Noegel, A. A. (1988) *Dev. Genet. (N.Y.) 9*, 521–530.
Simon, M.-N., Mutzel, R., Mutzel, H., & Veron, M. (1988) *Plasmid 19*, 94–102.
Spudich, J. A., & Watt, S. (1971) *J. Biol. Chem. 246*, 4866–4871.
Stossel, T. P. (1989) *J. Biol. Chem. 264*, 18261–18264.
Stossel, T. P., Chaponnier, C., Ezzell, R. M., Hartwig, J. H., Janmey, P. A., Kwiatkowski, D. J., Lind, S. E., Smith, D. B., Southwick, F. S., Yin, H. L., & Zaner, K. S. (1985) *Annu. Rev. Cell Biol. 1*, 353–402.
Vandekerckhove, J. (1990) *Curr. Opin. Cell Biol. 2*, 41–50.
Walsh, T. P., Weber, A., Davis, K., Bonder, E., & Mooseker, M. (1984) *Biochemistry 23*, 6099–6102.
Way, M., & Weeds, A. (1988) *J. Mol. Biol. 203*, 1127–1133.
Yin, H. L., & Stossel, T. P. (1979) *Nature 281*, 581–586.
Yin, H. L., Janmey, P. A., & Schleicher, M. (1990) *FEBS Lett. 264*, 78–80.

Inhibition of Myosin ATPase by Beryllium Fluoride†

Brigitte Phan and Emil Reisler*
Department of Chemistry and Biochemistry and Molecular Biology Institute, University of California, Los Angeles, California 90024

Received November 1, 1991; Revised Manuscript Received March 13, 1992

ABSTRACT: Inhibition of the myosin subfragment 1 (S-1) ATPase activity by beryllium fluoride was studied directly in the presence of MgATP and following preincubation of samples with MgADP. In both cases, the rates of inhibition were very slow, with k_{app} = 0.5 and 58 M^{-1} s^{-1}, respectively, in analogy to the rates of inhibition of myosin ATPase by vanadate [Goodno, C. C. (1979) *Proc. Natl. Acad. Sci. U.S.A. 76*, 2620–2624]. The very different rates of inhibition in the presence of MgATP and on preincubation with MgADP suggested that beryllium fluoride binds to the M·ADP state of myosin. The slow inhibition rates and the nonlinear dependence of the observed rates on beryllium fluoride concentration were consistent with a two-step inhibition process involving a rapid binding equilibrium to yield a collisional complex, M·ADP·BeF_3^-, and its slow isomerization into M*·ADP·BeF_3^-. A third, much slower, step was required to account for the conversion of the stable M*·ADP·BeF_3^- to a virtually irreversibly inhibited complex. Kinetic description of the inhibition pathway was derived from the observed rates of inhibition of myosin ATPase, information on the binding of beryllium fluoride to M·ADP, and measurements of ϵADP chase from M*·ϵADP·BeF_3^-. The isomerization rate and equilibrium constants were 1.4×10^{-2} s^{-1} and 50, respectively, and the overall binding constant of beryllium fluoride to M·ADP was 5×10^5 M^{-1}. The inhibitory complex showed a 16% enhancement to tryptophan fluorescence of S-1 and a reduced quenching of ϵADP by acrylamide. It is concluded that M*·ADP·BeF_3^- is analogous to the M*·ADP·V_i and M**·ADP·P_i states of myosin.

Muscles produce force by cyclic interactions between filaments of actin and myosin which are coupled to the hydrolysis of ATP. The simplified four-step scheme for myosin-catalyzed hydrolysis of ATP in the presence of Mg^{2+}, according to Bagshaw and Trentham (1973), is depicted in Scheme I where M, M*·ATP, M**·ADP·P_i, and M*·ADP represent conformational states of myosin–nucleotide complexes having distinct spectral properties. At room temperature, the predominant steady-state intermediate is the species M**·ADP·P_i. This transition state is believed to be a key intermediate in the energy transduction process (Johnson & Taylor, 1978). Thus, there is considerable interest in the characterization of the M**·ADP·P_i state and in developing appropriate probes for that purpose.

Scheme I

$$M + ATP \leftrightarrow M^*\cdot ATP \leftrightarrow M^{**}\cdot ADP\cdot P_i \leftrightarrow M^*\cdot ADP \leftrightarrow M + ADP$$

Vanadate, a well-known inorganic phosphate analogue [for a review, see Goodno (1982)], has been used extensively to characterize the M**·ADP·P_i state. In the presence of ADP, vanadate binds to the active site of myosin and forms an inactive ternary complex, M*·ADP·V_i. As suggested by X-ray diffraction studies with glycerinated muscle (Goody et al., 1980) and spin-label experiments (Wells & Bagshaw, 1984), this complex is conformationally analogous to the intermediate M**·ADP·P_i species. However, the tendency of vanadate to polymerize and its absorption in the UV region significantly limit its use. Therefore, additional phosphate analogues would facilitate further characterization of the M**·ADP·P_i state of myosin.

The complexes of aluminum and beryllium with fluoride, AlF_4^- and BeF_3^-, belong to a relatively new class of phosphate analogues which affect the activities of several G proteins (Bigay et al., 1987), phosphatases (Lange et al., 1986), and ATPases (Robinson et al., 1986). Recently, AlF_4^- and BeF_3^- were shown to bind to the catalytic sites of the beef F_1-ATPase with a stoichiometry of one metal per catalytic site and to inhibit the F_1-ATPase (Issartel et al., 1991). The essentially

† This work was supported by Grant AR22031 and Atherosclerosis Training Grant HL 07386 from the National Institutes of Health and by Grant DMB 89-05363 from the National Science Foundation.

0006-2960/92/0431-4787$03.00/0